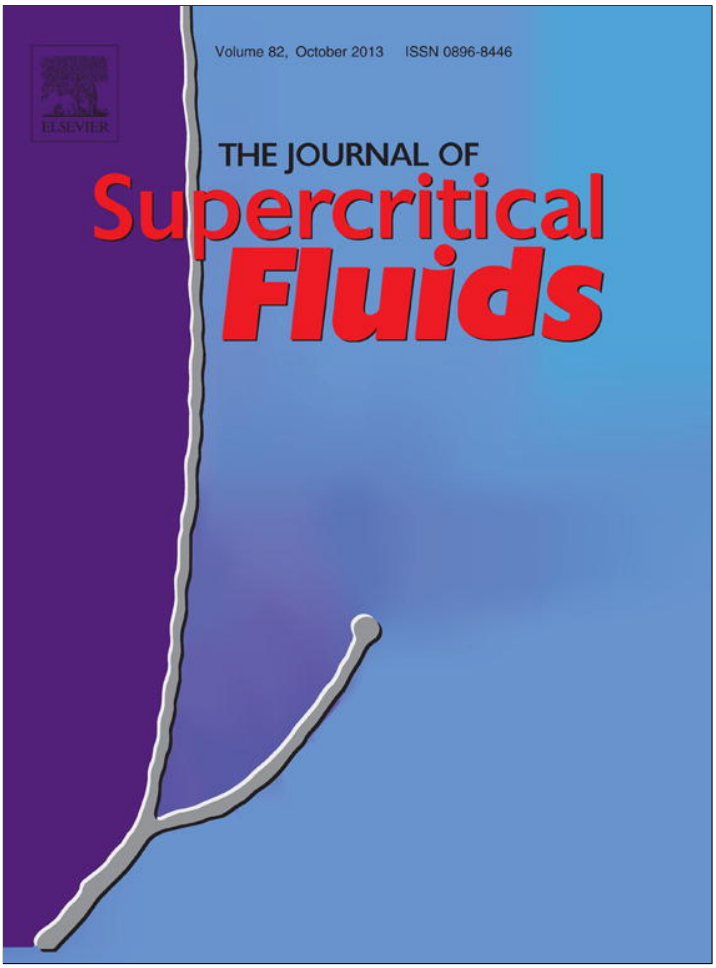

J. of Supercritical Fluids 82 (2013) 191–199

Contents lists available at ScienceDirect

The Journal of Supercritical Fluids

journal homepage: www.elsevier.com/locate/supflu

# Experimental measurements and modeling of $CO_2$ solubility in sunflower, castor and rapeseed oils

T. Regueira [a], P.J. Carvalho [b], M.B. Oliveira [b], L. Lugo [c], J.A.P. Coutinho [b], J. Fernández [a,*]

[a] Laboratorio de Propiedades Termofísicas, Departamento de Física Aplicada, Universidade de Santiago de Compostela, E1782 Santiago de Compostela, Spain
[b] CICECO, Departamento de Química, Universidade de Aveiro, 3810-193 Aveiro, Portugal
[c] Dpto. Física Aplicada, Edificio de Ciencias Experimentales, Universidade de Vigo, E-36310 Vigo, Spain

ARTICLE INFO

*Article history:*
Received 4 April 2013
Received in revised form 12 July 2013
Accepted 16 July 2013

*Keywords:*
Carbon dioxide
Vegetable oil
Solubility
High pressure
SRK EoS

ABSTRACT

In this work solubility measurements of $CO_2$ in three vegetable oils, a high oleic sunflower oil (HOSO), a castor oil and a rapeseed oil, for mole fractions ranging from 0.32 to 0.93 in the temperature range 298–363 K and up to 75 MPa were performed. Moreover, the densities and viscosities of these oils are reported from 278.15 to 373.15 K at atmospheric pressure. These data were used to evaluate the predictive ability of the fragment based approach. Solubility data were modeled by means of the SRK EoS and predicted employing the Carvalho and Coutinho correlation. Global average deviations inferior to 6% in $CO_2$ mole fraction composition were achieved with the SRK EoS and maximum percentage absolute average deviations of 13% in pressure were obtained using the Carvalho and Coutinho correlation.



## 1. Introduction

The environmental drive for the use of rapidly biodegradable oils as lubricants has been a gradual process in Europe and niche markets have arisen where mineral oils have been banned by legislation. Vegetable oils are an obvious choice, which can offer an optimum solution, particularly in total-loss systems (drilling muds, chain-saw bar oils and outboard engines) and partial-loss systems (hydraulic oils and greases). With the aid of selective plant breeding and additives, more thermal and oxidative stable vegetable oils can be formulated [1,2]. The commercial use of a vegetable-oil based system would represent a significant environmental improvement in areas where hydrocarbons are still employed [3–5].

The EU Ecolabel is a voluntary award system for the promotion of products with a reduced environmental impact during their life cycle. This scheme is part of the sustainable consumption and production policy of the European Community, which aims at substituting hazardous substances by safer ones, wherever technically possible [6]. The EU established in 2011 the latest ecological criteria for the award of the EU Ecolabel to lubricants. This product group comprises five categories that include hydraulic fluids and tractor transmission oils, greases and stern tube greases, chainsaw oils, concrete release agents, wire rope lubricants, stern tube oils and other total loss lubricants, two-stroke oils and industrial and marine gear oils [7].

Vegetable oils as lubricants are environmentally preferred to petroleum-based oils not only because they are renewable raw materials but also because they are biodegradable and non-toxic [8]. Other advantages include very low volatility due to the high molecular weight of the triglyceride molecule and excellent temperature-viscosity properties. Their polar ester groups are able to adhere to metal surfaces, and therefore, provide good lubricity. In addition, vegetable oils have high solubilizing power for polar contaminants and additive molecules [1]. However there are concerns about their oxidative stability and low-temperature performance. Improvements in oxidative stability can be made through chemical or genetic modifications [2,9–12], as well as adding antioxidant additives. [13,14]

Two-stroke engines are one of the applications where most of the lubricants and their degradation products are released directly into the environment, polluting the soil, water and atmosphere [15–17]. The knowledge of the solubility of different gases, such as $O_2$, $N_2$ and $CO_2$, in lubricants used for two stroke engines is important because these gases are involved in the combustion process together with the lubricant and the gasoline in the combustion chamber and this can provide information on the best lubricant choice. Moreover, $CO_2$ is a natural refrigerant that is being considered as a potential candidate to replace existing refrigerants, especially in small and medium systems [18]. Thus, in applications

* Corresponding author. Tel.: +34 881814046; fax: +34 881814112.
*E-mail addresses:* teresa.regueira@usc.es (T. Regueira), quijorge@ua.pt (P.J. Carvalho), mbelo@ua.pt (M.B. Oliveira), luis.lugo@uvigo.es (L. Lugo), jcoutinho@ua.pt (J.A.P. Coutinho), josefa.fernandez@usc.es, josefafdez@hotmail.es (J. Fernández).

0896-8446/$ – see front matter © 2013 Elsevier B.V. All rights reserved.
http://dx.doi.org/10.1016/j.supflu.2013.07.010

where the lubricant is in contact with the refrigerant, its solubility in the oil is a key property [19]. It is well recognized that the surrounding gas affects lubrication performance in any lubrication regimes. In hydrodynamic lubrication the surrounding gas and its pressure affect the dissolution of the gas into the lubricant, which may cause changes in the lubricant viscosity and may further cause degradation of the lubricant. Therefore, investigating the effects of the surrounding gas on lubrication is important to design the lubricant for reliability and safety [20]. Furthermore, the knowledge of the $CO_2$ + vegetable oil solubility data is necessary for the design of supercritical carbon dioxide oil extraction processes from seeds [21–24].

In this work solubility measurements of $CO_2$ in three vegetable oils susceptible of being used as lubricant base oils, a high oleic sunflower oil, a castor oil, and a rapeseed oil, were carried out in the temperature range 298.15–363.15 K and for pressures up to 75 MPa. It should be highlighted, that solubilities of $CO_2$ in a rapeseed oil were previously studied by Klein and Schulz [25] at 313.15, 333.15, 353.15 and 373.15 K and pressures up to 85 MPa. The present work is focused on different temperatures and also broadens the range to a lower temperature, i.e. 298.15 K. Data is also presented in a lower $CO_2$ composition range. Additionally, solubilities of $CO_2$ in castor oil were studied by Ndiaye et al. [26] in the temperature range from 308.15 to 343.15 K up to 25.5 MPa. Our experimental data broadens both temperature and pressure ranges up to 363.15 K and 74 MPa, respectively.

Additionally, in the present work, the SRK EoS was used to model the experimental solubility data, which were also used to evaluate the prediction ability of the Carvalho and Coutinho correlation [27]. Moreover, densities and viscosities of these oils were experimentally measured over a wide range of temperatures in order to perform a better characterization of the studied oils and also to analyze the reliability of the fragment based approach [28,29].

## 2. Materials and methods

High oleic sunflower oil (HOSO), castor oil and rapeseed oil were kindly provided by Verkol Lubricantes. Fatty acid composition of these oils was determined in the Instituto de la Grasa (CSIC, Seville) and is presented in Table 1, along with the respective standard deviation. Prior to the measurements, oils were dried under high vacuum (0.1 Pa) and at moderate temperature (around 353 K) for a period of 48 h. Carbon dioxide ($CO_2$) was provided by Air Liquide with a purity ≥ 99.998%, their $H_2O$, $O_2$, $C_nH_m$, $N_2$ and $H_2$ impurities volume fractions being lower than (3, 2, 2, 8 and 0.5) × $10^{-6}$, respectively. Molecular weights of the oils were estimated taking into account their fatty acid composition presented in Table 1. The obtained values are 881.77, 920.89 and 878.83 g $mol^{-1}$ for HOSO, castor oil and rapeseed oil, respectively.

Density and viscosity of the oils were measured at atmospheric pressure in an automated SVM 3000 Anton Paar rotational Stabinger apparatus [30]. The SVM 3000 uses Peltier elements for fast and efficient thermostatization. The temperature uncertainty is 0.02 K from 288.15 to 378.15 K and 0.05 K outside this range, whereas the uncertainty of the dynamic viscosity is 1%. This equipment has also a vibrating-tube that permits measurements of the densities with an uncertainty of 0.0005 g $cm^{-3}$. Measurements were performed from 278.15 to 373.15 K.

Solubility measurements were performed in a high pressure equilibrium cell based on the design of Daridon and co-workers [31,32] using the synthetic method which avoid the sampling and analyses of liquid and vapour phases. The high pressure equilibrium cell is a variable volume high pressure cell that consists of a horizontal hollow stainless steel cylinder, closed at one end by a movable piston and at the other end by a sapphire window that allows a visual observation of the interior of the pressure cell. The volume of this cell varies from 8 to 30 $cm^3$. Phase behavior as a function of temperature and pressure is observed by means of a video acquisition system, consisting of an endoscope and a video camera connected to a computer, which permits to follow the phase change inside the cell. The interior of the equilibrium cell is illuminated by an optical fibber through a second sapphire window located in the wall of the cell. A magnetic bar placed inside the cell and controlled by an external magnetic stirrer is used to homogenize the system. The internal temperature is kept constant by means of a thermostatic bath circulator. The temperature is measured with three-wire Pt100 thermometer (Bresimar, Aveiro), with an uncertainty of 0.15 K, connected to a calibrated platinum resistance inserted inside the cell close to the sample. The pressure is measured by a piezoresistive silicon pressure transducer (Kulite HEM 375) directly fixed inside the cell to reduce dead volumes. This transducer was previously calibrated and certified following the EN 837-1 standard and with accuracy better than 0.2% and the reproducibility of the pressure readings was 0.02 MPa. More details can be found in a previous work [33].

Measurements were performed in the temperature range from 298.15 to 363.15 K for the systems $CO_2$ + HOSO and $CO_2$ + rapeseed oil, whereas for the system $CO_2$ + castor oil measurements were performed in the temperature range from 323.15 to 363.15 K due to the high viscosity of castor oil at 298.15 K that hinders a proper homogenization of the system.

## 3. Models

### 3.1. Soave–Redlich–Kwong EoS

The Soave–Redlich–Kwong EoS [34] was used to model the experimental solubility data measured in this work. The SRK EoS, in terms of pressure is given by:

$$p = \frac{RT}{V_m - b} - \frac{a}{V_m(V_m + b)} \quad (1)$$

where $p$ is the pressure, $T$ is the temperature, $R$ is the gas constant, $V_m$ is the molar volume and $a$ is the pure component energy

**Table 1**
Fatty acid composition of high oleic sunflower oil (HOSO), castor oil and rapeseed oil, along with their standard deviations ($\sigma$).

| | HOSO | | Castor oil | | Rapeseed oil | |
|---|---|---|---|---|---|---|
| Fatty acid | % Mass fraction | $\sigma$ | % Mass fraction | $\sigma$ | % Mass fraction | $\sigma$ |
| Palmitic | 3.98 | 0.01 | 2.25 | 0.04 | 4.86 | 0.01 |
| Estearic | 2.99 | 0.02 | 2.50 | 0.06 | 1.65 | 0.05 |
| Oleic | 82.89 | 0.20 | 7.21 | 0.18 | 65.28 | 0.49 |
| Linoleic | 9.17 | 0.11 | 8.40 | 0.14 | 19.49 | 0.23 |
| Linolenic | – | – | – | – | 7.69 | 0.26 |
| Ricinoleic | – | – | 79.64 | 0.24 | – | – |
| Arachidic | 0.26 | 0.01 | – | – | 0.79 | 0.04 |
| Behenic | 0.72 | 0.04 | – | – | 0.26 | 0.01 |

parameter which has a Soave-type temperature dependency given by the following equation:

$$a = a_0\left[1 + c_1(1 - \sqrt{T_r})\right]^2 \quad (2)$$

where $T_r$ is the reduced temperature ($T/T_c$, where $T_c$ is the critical temperature). $a_0$ and $c_1$ are given by the following expressions:

$$a_0 = 0.42747\frac{R^2T_c^2}{p_c} \quad (3)$$

$$c_1 = 0.48 + 1.574\omega - 0.176\omega^2 \quad (4)$$

The pure compound co-volume parameter, $b$, is given by:

$$b = \frac{0.08664RT_c}{p_c} \quad (5)$$

where $p_c$ is the critical pressure and $\omega$ is the acentric factor.

When dealing with mixtures, the energy and co-volume parameters are calculated employing the conventional van der Waals one-fluid mixing rules,

$$a = \sum_i\sum_j x_i x_j a_{ij} \quad (6)$$

$$a_{ij} = \sqrt{a_i a_j}(1 - k_{ij}) \quad (7)$$

$$b = \sum_i\sum_j x_i x_j b_{ij} \quad (8)$$

$$b_{ij} = \sqrt{b_i b_j}(1 - l_{ij}) \quad (9)$$

There are two adjustable parameters from the solubility data for the studied mixtures, i.e. the binary interaction parameters $k_{ij}$ and $l_{ij}$. The objective function employed for the binary parameters regression was

$$OF = \sqrt{\frac{1}{N}\sum_i^N (x_i^{\text{exp.}} - x_i^{\text{cal.}})^2} \quad (10)$$

where $x_i$ is the mole fraction of component "$i$" in the phases selected in the optimization.

### 3.2. Carvalho and Coutinho correlation

Carvalho and Coutinho [27] have proposed the following general correlation for predicting the solubility of $CO_2$ in nonvolatile solvents:

$$p = m_{CO_2} e^{\left(6.8591 - \frac{2004.3}{T}\right)} \quad (11)$$

where $p$ is the pressure in MPa, $m_{CO_2}$ is the $CO_2$ solubility expressed in molality (mol kg$^{-1}$) and $T$ is the temperature in K. Eq. (11) is valid for pressures up to 5 MPa, for temperatures ranging from room temperature up to 363 K and molalities up to 3 mol kg$^{-1}$. This correlation infers that when the molecular weight effect is removed from the solubility analysis by comparing the solubilities expressed in molalities instead of in mole fractions, the solubility differences, among different systems are minimized and the solubility of $CO_2$ in nonvolatile solvents becomes essentially solvent independent.

## 4. Results and discussion

### 4.1. Density and viscosity of the pure oils

The densities and the dynamic viscosities were measured in the 278.15–373.15 K temperature range, at atmospheric pressure. The experimental values are depicted in Fig. 1 and presented in Table S1 in the supplementary data. These results complement those from literature. Thus, in the case of castor oil, up to our knowledge, density has been reported only from 298 to 333 K by Sankarappa et al. [35] and what concerns rapeseed oil, density and viscosity data have not been previously measured at 278.15 K. The rapeseed oil and HOSO have similar density and viscosity values whereas castor oil is the densest and also the most viscous. This behavior is due to the additional hydroxyl groups of the ricinoleic chains of the castor oil, which can form hydrogen bonds.

The percentage relative deviations between the experimental HOSO density data and those reported for HOSO [36,37] and sunflower oil [35,38,39] are presented in Fig. 2a. Agreement between our experimental density and viscosity data and those from literature has been quantified in terms of absolute average deviation (AAD%) which is given by:

$$AAD(\%) = \frac{100}{N}\sum_{i=1}^{N}\left|\frac{Y_i^{\text{exp}} - Y_i^{\text{ref}}}{Y_i^{\text{ref}}}\right| \quad (12)$$

and the *bias*%:

$$bias(\%) = \frac{100}{N}\sum_{i=1}^{N}\frac{Y_i^{\text{exp}} - Y_i^{\text{ref}}}{Y_i^{\text{ref}}} \quad (13)$$

where $N$ is the number of experimental data points and $Y_i^{\text{exp}}$ and $Y_i^{\text{ref}}$ represent the experimental and literature values, respectively. Concerning the information given by the *bias*%, it should be mentioned that, when AAD% = *bias*%, all the experimental points are higher than the literature data and if AAD% = −*bias*%, all the experimental densities are lower than the literature values [40].

Thus, our HOSO density data show an overall AAD% of 0.55% with literature data for HOSO [36,37] and sunflower oil [35,38,39]. We

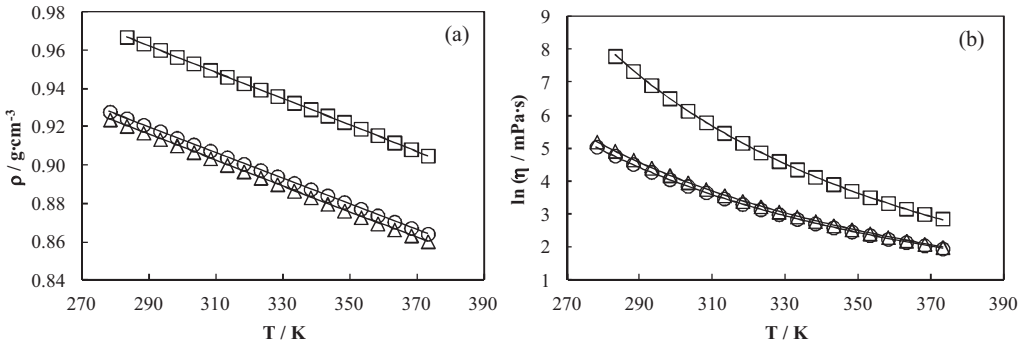


**Fig. 1.** (a) Experimental density and (b) viscosity values of the oils measured in this work. (□) Castor oil, (○) rapeseed oil and (△) HOSO. Lines represent correlations according to Eqs. (14) and (15) for density and viscosity values, respectively.

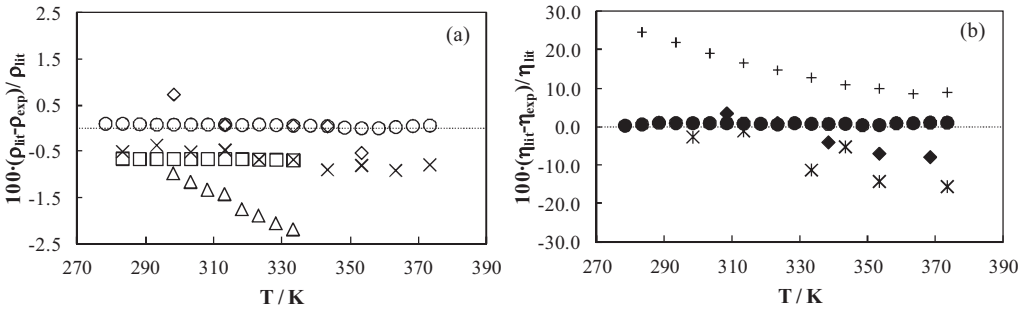


**Fig. 2.** (a) Comparison between the reported density data of HOSO and values from literature for HOSO (Quinchia et al. [37] (◊) and Regueira et al. [36] (○)) and for sunflower oil (Esteban et al. [38] (×), Sankarappa et al. [35] (△) and Guignon et al. [39] (□)). (b) Comparison between the reported viscosity data of HOSO and values from literature for HOSO (Regueira et al. [36] (●) and Quinchia et al. [42] (∗)) and for sunflower oil (Fasina et al. [43] (⧫) and Esteban et al. [38] (+)).

**Table 2**
Parameters of the polynomial density correlation (Eq. 14) for the vegetable oils.

| | $a_0$ g cm$^{-3}$ | $10^3\,a_1$ g cm$^{-3}$ K$^{-1}$ | $10^7\,a_2$ g cm$^{-3}$ K$^{-2}$ | $10^{10}\,a_3$ g cm$^{-3}$ K$^{-3}$ | $10^4\,\sigma$ g cm$^{-3}$ |
|---|---|---|---|---|---|
| HOSO | 0.96336 | 0.7519 | −45.553 | 48.192 | 1.4 |
| Castor oil | 1.37463 | −2.6617 | 60.723 | −61.982 | 1.0 |
| Rapeseed oil | 1.12203 | −0.7073 | 0.0840 | 0.9028 | 1.2 |

**Table 3**
Parameters of the VFT equation (Eq. (15)) for the vegetable oils.

| | $A$ | $B$/K | $T_0$/K | $10^2\,\sigma$ |
|---|---|---|---|---|
| HOSO | −2.171884 | 908.218 | 155.0831 | 0.2 |
| Castor oil | −3.343743 | 1247.729 | 171.3842 | 1.2 |
| Rapeseed oil | −2.097011 | 886.062 | 154.1951 | 0.1 |

have found *bias*% values different from AAD% for one data series and *bias*% = |AAD%| for four sets (one of them positive). Furthermore, the density obtained for the castor oil was compared with those published by Sankarappa et al. [35] showing an AAD% of 0.98%, the AAD% being equal to the *bias*%. Finally, the rapeseed oil density was compared with those of the 48 samples measured at 293 K by Wesołowski and Erecińska [41], showing an AAD% of 0.80%, and with those reported by Esteban et al. [38] in the 283.15–373.15 K temperature range, showing an AAD% of 0.19%. For these last data sets the AAD% are different from the *bias*%.

The viscosity of HOSO was compared with literature values of HOSO [36,42] and sunflower oil [38,43], as depicted in Fig. 2b, showing an overall *bias*% of 2.6% and an overall AAD% of 5.9%. Besides, the castor oil viscosity values were also compared with those reported in literature [42,44,45], finding an overall *bias*% of 2.9% and an AAD% of 10%. Finally, the rapeseed oil viscosity values were compared with reported literature values [38,43,46] yielding an overall *bias*% of −2.5% and a global AAD% of 8.4%.

The high deviations found with some of the literature data for the oils densities and viscosities can be explained by the different fatty acid composition of the oil samples, particularly in the case of sunflower oil and HOSO. Sunflower oil from Esteban et al. [38] has a composition of only 38.7% in oleic acid whereas our sunflower oil has 83%. Guignon et al. [39] and Sankarappa et al. [35] do not report the sunflower oil compositions.

Density values were correlated as a function of temperature by means of a polynomial, as follows:

$$\rho = a_0 + a_1 T + a_2 T^2 + a_3 T^3 \tag{14}$$

where $\rho$ is the density in g cm$^{-3}$ and $T$ is the temperature in K.

The parameters of the density adjustment are presented in Table 2 along with the standard deviations ($\sigma$).

The viscosity values were correlated as function of temperature by the Vogel–Fulcher–Tammann (VFT) equation:

$$\ln(\eta) = A + \frac{B}{T - T_0} \tag{15}$$

where $\eta$ is the dynamic viscosity in mPa s.

The parameters obtained by fitting the VFT equation against the experimental data are presented in Table 3 along with standard deviations ($\sigma$) of the fit.

The fragment based approach for estimating thermophysical properties of fats and vegetable oils [28,29] was tested to predict the density values of the studied oils. This methodology adopts a chemical constituent fragment-based approach to estimate the triglyceride pure component properties from fragment composition and parameters of the fragments. The fragment-specific parameters were obtained by Zong et al. [28,29] by regressing against very limited experimental data for triglycerides. According to this method, the liquid molar volume of triglycerides can be calculated according to the following equation:

$$V^l = \sum_A N_{frag,A} V_A^l(T) \tag{16}$$

where $V_A^l$ is the liquid molar volume contribution of fragment $A$ and $N_{frag,A}$ is the number of fragments $A$ in the component. The temperature dependency for the liquid molar volume of fragment $A$ is given by [28,29]:

$$V_A^l = \frac{1 + B_{2,A} T}{B_{1,A}} \tag{17}$$

where $B_{1,A}$ and $B_{2,A}$ are the temperature dependency correlation parameters of fragment $A$. This method [28] predicts the density values reported in Table S1 with percentage absolute average deviations (AAD%) of 0.8% for HOSO and 1.1% for rapeseed oil. For the castor oil, the authors [28] do not provide parameters for the

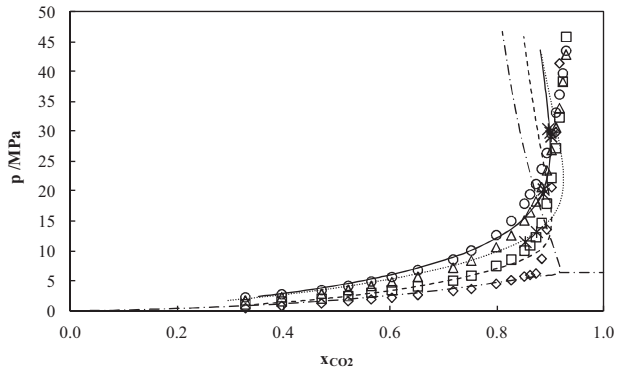


**Fig. 3.** Experimental solubility data of the system $CO_2$ + HOSO at 298 K (◊), 323 K (□), 348 K (△) and 363 K (○). Data from Fernández-Ronco et al. [47] for the system $CO_2$ + sunflower oil at 325.9 K (∗). Lines represent the SRK EoS with two interaction parameters ($k_{ij}$ and $l_{ij}$) from Table 8 at 298 K (–·–), 323 K (– –), 348 K (. . .) and 363 K (—).

ricinoleic fragment. We have calculated the values of these parameters, $B_{1,A}$ and $B_{2,A}$, finding a value of 4.27 kmol m$^{-3}$ for $B_{1,A}$ and of $1.2485 \times 10^{-4}$ K$^{-1}$ for $B_{2,A}$ with an AAD% of 0.03%.

Additionally, the fragment based approach [28,29] was also employed to estimate the viscosity of the studied vegetable oils. Through this approach, the triglycerides liquid viscosities can be calculated from the viscosity fragment composition and fragment-specific parameters according to the equation:

$$\ln \eta = \sum_{A} N_{frag,A} \ln \eta_A(T) \tag{18}$$

where $\ln\eta_A$ represents the liquid viscosity contribution of the fragment $A$ (expressed in units of Pa s) and $N_{frag,A}$ is the number of fragments $A$ in the component.

The expression for the liquid viscosity contribution of fragment $A$, as a function of temperature is the following:

$$\ln \eta_A = C_{1,A} + \frac{C_{2,A}}{T} + C_{3,A} \ln T \tag{19}$$

where $C_{1,A}$, $C_{2,A}$ and $C_{3,A}$ represent temperature dependency correlation parameters for viscosity. AADs% of 3.6% and 4.0% for the viscosity prediction of HOSO and rapeseed oil, respectively, were obtained using this correlation. These uncertainties are quite low, i.e. the values of the parameters are reliable. For the castor oil, parameters for the ricinoleic fragment are not available [28]. Thus, we have calculated the parameters for viscosity prediction for the ricinoleic fragment, using our experimental viscosity data, finding the following values for the parameters: −129.17 Pa s for $C_{1,A}$, 7269.3 K for $C_{2,A}$ and 32.471 K for $C_{3,A}$ with an AAD% of 0.38%.

### 4.2. Experimental solubility data

Experimental solubility data are presented in Tables 4–6 for the three systems studied whereas the $p$-$x$ diagrams are depicted in Figs. 3–5. The temperature increase leads to an increase on the equilibrium pressure up to a crossing point that is observed for all the systems. These crossing of isotherms are located at ($w_{CO_2}$, $p$) around 0.31, 21 MPa, 0.26, 28 MPa, and 0.32, 25 MPa for the systems $CO_2$ + HOSO, $CO_2$ + castor oil and $CO_2$ + rapeseed oil, respectively. Above this point the temperature dependency of the solubility is inversed, increasing with the temperature increase. Crossovers of the isotherms for these systems have been previously reported by Klein and Schulz [25] for $CO_2$ + rapeseed oil and also by Ndiaye et al. [26] for $CO_2$ + castor oil. The solubility data for the $CO_2$ + HOSO system were measured for $CO_2$ mass fractions up to 0.40 and 61 MPa and are depicted in Fig. 3 along with the values for the $CO_2$ + a sunflower oil system, reported by Fernández-Ronco et al. [47] at 325.9 K. The solubility data for the $CO_2$ + castor oil system were determined for $CO_2$ mass fractions up to 0.35 and 74 MPa and are depicted in Fig. 4, along with the literature solubility $CO_2$ data in

**Table 4**
Solubility data of the system $CO_2$ + HOSO.

| $w_{CO_2}$ | $T$/K | $p$/MPa | $w_{CO_2}$ | $T$/K | $p$/MPa |
|---|---|---|---|---|---|
| 0.024 | 298.34 | 0.519 | 0.024 | 348.39 | 1.800 |
| 0.032 | 298.10 | 0.879 | 0.032 | 348.20 | 2.338 |
| 0.042 | 298.27 | 1.294 | 0.042 | 347.95 | 2.934 |
| 0.051 | 298.31 | 1.681 | 0.051 | 348.05 | 3.570 |
| 0.060 | 297.88 | 1.978 | 0.060 | 347.94 | 4.226 |
| 0.070 | 298.39 | 2.247 | 0.070 | 347.96 | 4.858 |
| 0.085 | 298.05 | 2.699 | 0.085 | 347.90 | 5.749 |
| 0.112 | 298.01 | 3.378 | 0.112 | 348.20 | 7.271 |
| 0.130 | 298.02 | 3.722 | 0.130 | 348.23 | 8.470 |
| 0.164 | 298.39 | 4.579 | 0.164 | 348.19 | 10.70 |
| 0.191 | 297.92 | 5.189 | 0.191 | 348.06 | 12.68 |
| 0.220 | 298.03 | 5.800 | 0.220 | 348.24 | 15.18 |
| 0.235 | 298.48 | 6.046 | 0.235 | 348.14 | 16.57 |
| 0.253 | 297.96 | 6.310 | 0.253 | 348.37 | 18.36 |
| 0.273 | 298.39 | 8.762 | 0.273 | 348.36 | 20.75 |
| 0.292 | 298.36 | 13.67 | 0.292 | 348.23 | 23.57 |
| 0.312 | 298.39 | 20.71 | 0.312 | 348.04 | 26.96 |
| 0.333 | 298.49 | 29.93 | 0.333 | 348.36 | 30.76 |
| 0.352 | 298.00 | 41.48 | 0.352 | 348.22 | 34.00 |
| 0.372 | 298.17 | 60.92 | 0.372 | 348.44 | 38.38 |
| 0.024 | 323.18 | 1.130 | 0.392 | 348.21 | 42.98 |
| 0.032 | 323.16 | 1.630 | 0.024 | 362.92 | 2.310 |
| 0.042 | 323.35 | 2.090 | 0.032 | 362.87 | 2.824 |
| 0.051 | 323.26 | 2.523 | 0.042 | 363.27 | 3.528 |
| 0.060 | 323.15 | 3.077 | 0.051 | 363.21 | 4.236 |
| 0.070 | 323.44 | 3.532 | 0.060 | 363.14 | 4.976 |
| 0.085 | 323.29 | 4.175 | 0.070 | 362.92 | 5.716 |
| 0.112 | 323.03 | 5.115 | 0.085 | 363.21 | 6.880 |
| 0.130 | 323.22 | 5.958 | 0.112 | 362.98 | 8.636 |
| 0.164 | 323.55 | 7.555 | 0.130 | 363.20 | 10.15 |
| 0.191 | 323.30 | 8.631 | 0.164 | 363.21 | 12.73 |
| 0.220 | 323.35 | 10.14 | 0.191 | 363.24 | 15.11 |
| 0.235 | 323.33 | 11.01 | 0.220 | 363.26 | 18.00 |
| 0.253 | 323.34 | 12.37 | 0.235 | 363.31 | 19.57 |
| 0.273 | 323.14 | 14.75 | 0.253 | 363.11 | 21.28 |
| 0.292 | 323.33 | 18.00 | 0.273 | 363.11 | 23.81 |
| 0.312 | 323.16 | 22.31 | 0.292 | 363.25 | 26.48 |
| 0.333 | 323.08 | 27.28 | 0.312 | 363.21 | 29.68 |
| 0.352 | 323.03 | 32.42 | 0.333 | 363.52 | 33.24 |
| 0.372 | 323.02 | 38.47 | 0.352 | 363.34 | 36.26 |
| 0.392 | 323.45 | 45.93 | 0.372 | 363.19 | 39.82 |
| | | | 0.392 | 363.14 | 43.60 |

**Table 5**
Solubility data of the system $CO_2$ + castor oil.

| $w_{CO_2}$ | $T$/K | $p$/MPa | $w_{CO_2}$ | $T$/K | $p$/MPa |
|---|---|---|---|---|---|
| 0.024 | 323.46 | 1.506 | 0.240 | 348.45 | 23.94 |
| 0.061 | 323.30 | 3.645 | 0.260 | 348.31 | 28.46 |
| 0.101 | 322.93 | 5.633 | 0.293 | 348.30 | 36.66 |
| 0.130 | 323.45 | 7.198 | 0.309 | 348.45 | 40.15 |
| 0.150 | 323.31 | 8.337 | 0.334 | 348.29 | 47.00 |
| 0.190 | 323.20 | 11.06 | 0.350 | 348.00 | 52.34 |
| 0.221 | 323.22 | 15.47 | 0.024 | 363.39 | 2.449 |
| 0.240 | 323.28 | 20.85 | 0.061 | 363.41 | 5.673 |
| 0.260 | 323.32 | 27.35 | 0.101 | 363.15 | 9.167 |
| 0.293 | 323.39 | 40.99 | 0.130 | 363.30 | 11.87 |
| 0.309 | 323.16 | 46.30 | 0.150 | 363.12 | 13.75 |
| 0.334 | 323.46 | 58.91 | 0.190 | 363.06 | 18.24 |
| 0.350 | 323.27 | 73.97 | 0.221 | 363.29 | 22.74 |
| 0.024 | 348.23 | 2.197 | 0.240 | 363.17 | 26.20 |
| 0.061 | 348.25 | 4.919 | 0.260 | 363.35 | 30.28 |
| 0.101 | 348.19 | 7.796 | 0.293 | 363.36 | 37.29 |
| 0.130 | 348.45 | 10.25 | 0.309 | 363.14 | 40.18 |
| 0.150 | 348.38 | 11.74 | 0.334 | 363.23 | 46.08 |
| 0.190 | 348.22 | 15.78 | 0.350 | 363.31 | 50.24 |
| 0.221 | 348.35 | 19.94 | | | |

**Table 6**
Solubility data of the system $CO_2$ + rapeseed oil.

| $w_{CO_2}$ | $T$/K | $p$/MPa | $w_{CO_2}$ | $T$/K | $p$/MPa |
|---|---|---|---|---|---|
| 0.024 | 298.25 | 0.585 | 0.024 | 348.45 | 1.779 |
| 0.062 | 298.15 | 1.938 | 0.062 | 348.25 | 4.338 |
| 0.104 | 298.25 | 3.230 | 0.104 | 348.15 | 7.049 |
| 0.131 | 298.15 | 3.932 | 0.131 | 348.05 | 8.718 |
| 0.161 | 298.25 | 4.708 | 0.161 | 348.15 | 10.82 |
| 0.200 | 298.15 | 5.594 | 0.200 | 348.15 | 13.68 |
| 0.246 | 298.15 | 6.476 | 0.246 | 348.15 | 18.35 |
| 0.280 | 298.25 | 11.83 | 0.280 | 348.05 | 22.73 |
| 0.301 | 298.25 | 17.66 | 0.301 | 348.25 | 26.14 |
| 0.320 | 298.15 | 25.47 | 0.320 | 348.15 | 29.29 |
| 0.345 | 298.15 | 36.31 | 0.345 | 348.15 | 33.84 |
| 0.372 | 298.15 | 58.03 | 0.372 | 348.14 | 39.59 |
| 0.024 | 323.25 | 1.183 | 0.390 | 348.35 | 44.02 |
| 0.062 | 323.35 | 3.113 | 0.024 | 363.45 | 2.119 |
| 0.104 | 323.25 | 5.046 | 0.062 | 363.25 | 5.077 |
| 0.131 | 323.15 | 6.207 | 0.104 | 363.35 | 8.278 |
| 0.161 | 323.15 | 7.567 | 0.131 | 363.15 | 10.26 |
| 0.200 | 323.15 | 9.269 | 0.161 | 363.15 | 12.73 |
| 0.246 | 323.15 | 12.38 | 0.200 | 363.15 | 16.19 |
| 0.280 | 323.25 | 17.06 | 0.246 | 363.15 | 21.32 |
| 0.301 | 323.15 | 21.12 | 0.280 | 363.05 | 25.89 |
| 0.320 | 323.05 | 25.35 | 0.301 | 363.15 | 29.02 |
| 0.345 | 323.05 | 31.55 | 0.320 | 363.05 | 31.84 |
| 0.372 | 323.05 | 39.80 | 0.345 | 363.05 | 35.97 |
| 0.390 | 323.05 | 47.58 | 0.372 | 363.05 | 40.86 |
| | | | 0.390 | 363.05 | 44.60 |

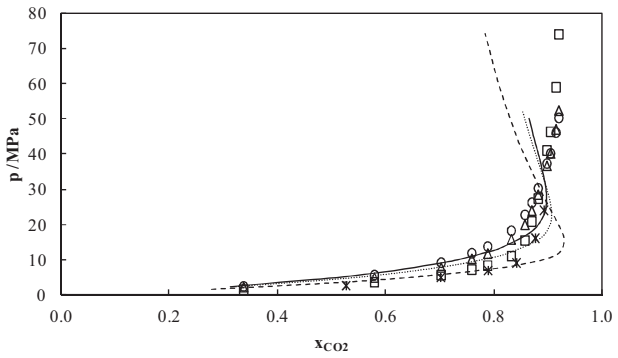


**Fig. 4.** Experimental solubility data of the system $CO_2$ + castor oil at 323 K (□), 348 K (△) and 363 K (○). Data from Ndiaye et al. [26] for the system $CO_2$ + castor oil at 323.15 K (∗). Lines represent the SRK EoS with two interaction parameters ($k_{ij}$ and $l_{ij}$) from Table 8 at 323 K (– –), 348 K (. . .) and 363 K (—).

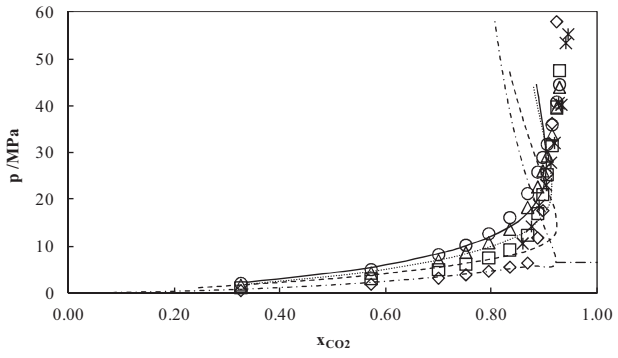


**Fig. 5.** Experimental solubility data of the system $CO_2$ + rapeseed oil at 298 K (◊), 323 K (□), 348 K (△) and 363 K (○). Data from Klein and Schulz [25] at 333 K (∗). Lines represent the SRK EoS with two interaction parameters ($k_{ij}$ and $l_{ij}$) from Table 8 at 298 K (–·–), 323 K (– –), 348 K (. . .) and 363 K (—).

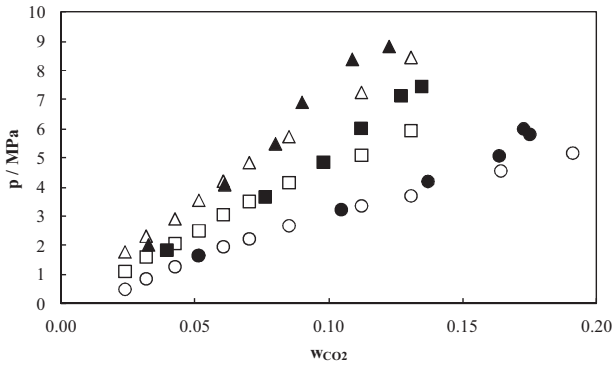


**Fig. 6.** Solubility of $CO_2$ in HOSO (empty symbols) and in BIO-2T-03 [48] (filled symbols) at 298 K (○, ●), 323 K (□, ■) and 348 K (△, ▲).

other castor oil reported by Ndiaye et al. [26] at 323.15 K. This figure shows that our values at this temperature are in agreement with those from Ndiaye et al. [26] Also, it must be noted that other isotherms (different from the ones studied in the present work, i.e. 313.15, 333.15 and 343.15 K) were reported by Ndiaye et al. [26] for this system but they were not plotted to avoid a misleading figure. The solubility data for the $CO_2$ + rapeseed oil system measured for $CO_2$ mass fractions up to 0.39 and 58 MPa are depicted in Fig. 5, along with the solubility data reported by Klein und Schulz [25] at 333.15 K. These last authors have also reported solubility data for this system at 313.15, 353.15 and 373.15 K. A good agreement is found between the experimental data and those available in the literature at a single temperature, taking into account that fatty acid composition of the oils is not the same for the compared samples. In a previous work we have reported the $CO_2$ solubility in a HOSO-based lubricant [48], BIO-2T-03. Interestingly, and despite the composition differences inherent to the two oils, the $CO_2$ solubility in both is remarkably similar, as depicted in Fig. 6.

In Fig. 7a comparison between the solubility of the $CO_2$ in the different oils in mole and mass fraction, at 323 K, is presented. The solubilities up to a $CO_2$ mass fraction of 0.2 are similar in the three of them. Over this composition, $CO_2$ solubility starts to increase slower for the three oils, keeping similar values in HOSO and in the rapeseed oil, whereas in the castor oil the $CO_2$ solubilities are lower. This is likely due to the hydroxyl groups of the ricinolecic chains of the castor molecule, which are not present in the other two oils. However, when solubility is expressed in mass fraction, the solubility curve of the system $CO_2$ + castor oil is closer to the other systems, but still having lower solubility values. Carvalho and Coutinho [27] have recently investigated the behavior of the $CO_2$ solubility in several solvents, among them alcohols, indicating that in spite of the strong $CO_2 \cdots OH$ interactions observed spectroscopically [49–53], the alcohol systems are the only ones with positive deviations to ideality (Raoult's Law). According to these authors, for this type of mixtures strong solute-solvent interactions are not enough to guarantee enhanced solubility if the solvent-solvent interactions destroyed during the solvation of the solute are not energetically compensated by that process.

### 4.3. SRK EoS modeling

The SRK EoS was here applied to describe the experimental solubility data and modeling was performed through the PE 2000 software [54]. The critical properties and acentric factor needed to apply the SRK EoS were obtained for the oils by the Constantinou and Gani group contribution method [55,56]. This method uses first and second order group contributions to distinguish special configurations such as isomers and was already previously used to

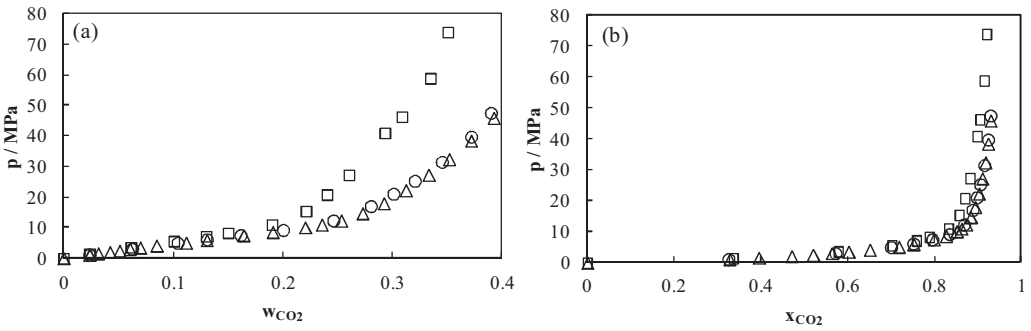


**Fig. 7.** Experimental solubility values (a) in mass fraction and (b) in mole fraction of the systems $CO_2$ + castor oil (□), $CO_2$ + HOSO (△) and $CO_2$ + rapeseed oil (○) at 323 K.

**Table 7**
Critical temperatures, pressures and acentric factors for oils estimated using the group contribution method of Constantinou and Gani [55,56].

| Oil | $T_c$/K | $p_c$/MPa | $\omega$ |
|---|---|---|---|
| HOSO | 974.55 | 0.33 | 1.99 |
| Castor oil | 961.57 | 0.35 | 1.94 |
| Rapeseed oil | 973.98 | 0.34 | 1.98 |

estimate critical properties of triglycerides [57]. The estimated oil critical properties and acentric factors are presented in Table 7.

Temperature dependent binary interaction parameters ($k_{ij}$ and $l_{ij}$) were employed for the SRK EoS solubility data description within the equation of state framework. Two different approaches were performed for modeling, one of them consists on adjusting only the $k_{ij}$, i.e. $l_{ij} = 0$, and the other one on adjusting both parameters. The use of two binary interaction parameters (Table 8) gives rise to better modeling results for all the systems in comparison with the use of only one parameter (Table S2). In Figs. 3–5 experimental solubility data together with SRK EoS and parameters of Table 8 were plotted for all systems. Global average deviations lower than 6% were obtained in the whole experimental temperature and pressure range using the two binary interaction parameters (Table 8). For all the systems and temperatures, positive binary interaction parameters are obtained. It is important to highlight that the SRK EoS, with the parameters of Table 8, predicts the existence of VLLE at 298.15 K for the system $CO_2$ + HOSO at $p = 6.45$ MPa from $x_{CO_2} = 0.916$ and for the system $CO_2$ + rapeseed oil at $p = 6.45$ MPa from $x_{CO_2} = 0.922$. This behavior was not experimentally investigated.

**Table 8**
Values of $k_{ij}$ and $l_{ij}$, and SRK EoS AAD% in $x_{CO2}$ for the $CO_2$ + oil systems modeled using two binary interaction parameters.

| Oil | $T$/K | $k_{ij}$ | $l_{ij}$ | AAD % |
|---|---|---|---|---|
| HOSO | 298.15 | 0.0435 | 0.0200 | 7.3 |
| | 323.15 | 0.0598 | 0.0297 | 2.5 |
| | 348.15 | 0.0528 | 0.0115 | 4.9 |
| | 363.15 | 0.0722 | 0.0200 | 2.3 |
| Global AAD% | | | | 4.3 |
| Castor oil | 323.15 | 0.0436 | 0.0059 | 7.6 |
| | 348.15 | 0.0612 | 0.0103 | 4.1 |
| | 363.15 | 0.0710 | 0.0104 | 3.6 |
| Global AAD % | | | | 5.1 |
| Rapeseed oil | 298.15 | 0.0418 | 0.0226 | 5.8 |
| | 323.15 | 0.0449 | 0.0082 | 6.5 |
| | 348.15 | 0.0590 | 0.0182 | 2.7 |
| | 363.15 | 0.0714 | 0.0213 | 2.2 |
| Global AAD % | | | | 4.3 |

### 4.4. Carvalho and Coutinho model

In Fig. 8 experimental solubility values are presented for the three systems along with the predictions obtained from Carvalho and Coutinho correlation [27] for all the temperatures studied and $CO_2$ molalities ($m_{CO_2}$) up to 5 mol kg$^{-1}$. The obtained AAD% in pressure was 11% for the system $CO_2$ + HOSO and 10% for the system $CO_2$ + rapeseed oil, whereas for the system $CO_2$ + castor oil the AAD% was 13%. It can be considered that the goodness of these predictions

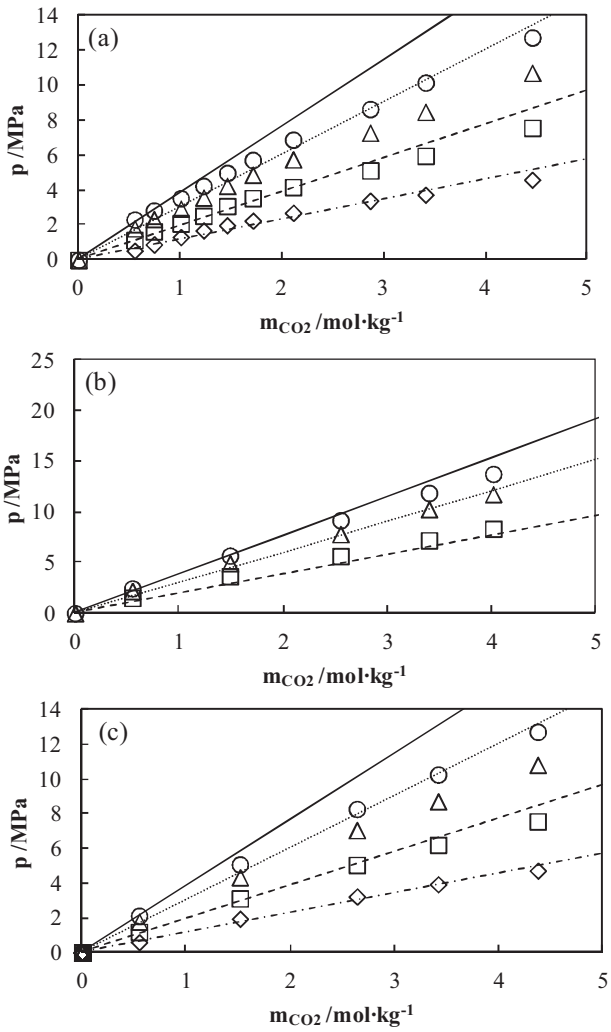


**Fig. 8.** Experimental solubility values of $CO_2$ in (a) HOSO, (b) castor oil and (c) rapeseed oil. Lines represent the Carvalho and Coutinho model [27]. 298 K (◊, –·–), 323 K (□, – –), 348 K (△, . . .) and 363 K (○, —).

are quite good although we had previously [48] obtained a slightly better prediction result (AAD% = 8.3%) for the system $CO_2$ + BIO-2T-3 with this model.

## 5. Conclusions

Density, viscosity and $CO_2$ solubility were determined for three vegetable oils, a high oleic sunflower oil (HOSO), castor oil and rapeseed oil. The rapeseed oil and HOSO present similar density and viscosity values whereas castor oil present both higher density as well as viscosity. A fragment based approach was employed for density and viscosity prediction of the oils in the whole experimental temperature range. This approach was able to predict the density of HOSO and rapeseed oil within an AAD% lower or equal to 1.1%. For the viscosity the fragment approach was able to predict within an AAD% of 3.6% for HOSO and 4.0% for rapeseed oil. Additionally, we have proposed parameters for the ricinoleic fragment to be employed in the fragment base approach for density and viscosity predictions.

HOSO and rapeseed oil present similar $CO_2$ solubilities in all the composition range. For $CO_2$ mass fraction higher that 0.2, the solubilities start to increase slower especially for castor oil, because of the hydroxyl groups of the ricinoleic chains of the later.

The experimental solubility data were described with the SRK EoS, with mole fraction global average deviations inferior to 6%. Furthermore, the Carvalho and Coutinho correlation predicts quite successfully the solubility data, up to molalities of 5 mol $kg^{-1}$ within an AAD%, in pressure, of 11% for the $CO_2$ + HOSO, 10% for the $CO_2$ + rapeseed oil system and 13% for the $CO_2$ + castor oil system.

## Acknowledgments

This work was carried out within the framework of the strategic and singular project "Biolubricants based on vegetable oils and their synthetic derivatives", which was funded by Spanish Science and Innovation Ministry and the EU FEDER program (PSE-320100-2006-1, PSE-420000-2008-4). We are very grateful to Verkol Lubricantes and Instituto de la Grasa (CSIC, Seville) for providing us the oil samples and the analysis of their fatty acid composition. Luis Lugo acknowledges the financial support from the Ramon y Cajal Program (Science and Innovation Ministry, Spain). Teresa Regueira acknowledges financial support provided by the FPU program (Ministry of Education, Culture and Sport, Spain). Part of this work was also funded by FCT – *Fundação para a Ciência e a Tecnologia*, through project Pest-C/CTM/LA0011/2011. Mariana B. Oliveira and Pedro J. Carvalho acknowledge the financial support from FCT – *Fundação para a Ciência e a Tecnologia* through their post-doctoral grants (SFRH/BPD/71200/2010, SFRH/BPD/82264/2011).

## Appendix A. Supplementary data

Supplementary data associated with this article can be found, in the online version, at http://dx.doi.org/10.1016/j.supflu.2013.07.010.

## References

[1] S.Z. Erhan, B.K. Sharma, J.M. Perez, Oxidation and low temperature stability of vegetable oil-based lubricants, Industrial Crops and Products 24 (2006) 292–299.
[2] J.M. Fernández-Martínez, M. Mancha, J. Osorio, R. Garcés, Sunflower mutant containing high levels of palmitic acid in high oleic background, Euphytica 97 (1997) 113–116.
[3] P. Miles, Synthetics versus vegetable oils: applications, options, and performance, J. Synthetic Lubrication 15 (1998) 43–52.
[4] B.J. Bremmer, L. Plonsker, Bio-Based Lubricants. A Market Opportunity Study Update, Omni Tech International, Ltd, Midland, United Soybean Board, 2008.
[5] L.A.T. Honary, An investigation of the use of soybean oil in hydraulic systems, Bioresource Technology 56 (1996) 41–47.
[6] Regulation (EC) No 66/2010 of the European Parliament and of the Council of 25 November 2009 on the EU Ecolabel, Official Journal of the European Union (2010), L 27/01–L 27/27.
[7] Commission decision of 24 June 2011 on establishing the ecological criteria for the award of the EU Ecolabel to lubricants, Official Journal of the European Union (2011), L 169/128–L 169/169.
[8] N.S. Battersby, S.E. Pack, R.J. Watkinson, A correlation between the biodegradability of oil products in the CEC L-33-T-82 and modified Sturm tests, Chemosphere 24 (1992) 1989–2000.
[9] W. Castro, J.M. Perez, S.Z. Erhan, F. Caputo, A study of the oxidation and wear properties of vegetable oils: soybean oil without additives, J. American Oil Chemists' Society 83 (2006) 47–52.
[10] R. Garcés, E. Martínez-Force, J.J. Salas, Vegetable oil basestocks for lubricants, Grasas y Aceites 62 (2011) 21–28.
[11] T.A. Isbell, B.A. Lowery, S.S. DeKeyser, M.L. Winchell, S.C. Cermak, Physical properties of triglyceride estolides from lesquerella and castor oils, Industrial Crops and Products 23 (2006) 256–263.
[12] G. Márquez-Ruiz, R. Garcés, M. León-Camacho, M. Mancha, Thermoxidative stability of triacylglycerols from mutant sunflower seeds, J. American Oil Chemists' Society 76 (1999) 1169–1174.
[13] R. Becker, A. Knorr, An evaluation of antioxidants for vegetable oils at elevated temperatures, Lubrication Science 8 (1996) 95–117.
[14] N.J. Fox, G.W. Stachowiak, Vegetable oil-based lubricants – a review of oxidation, Tribology International 40 (2007) 1035–1046.
[15] O.N. Anand, V.K. Chhibber, Vegetable oil derivatives: environment-friendly lubricants and fuels, J. Synthetic Lubrication 23 (2006) 91–107.
[16] S.Z. Erhan, S. Asadauskas, Lubricant basestocks from vegetable oils, Industrial Crops and Products 11 (2000) 277–282.
[17] M.P. Schneider, Plant-oil-based lubricants and hydraulic fluids, J. Science of Food and Agriculture 86 (2006) 1769–1780.
[18] M.-H. Kim, J. Pettersen, C.W. Bullard, Fundamental process and system design issues in $CO_2$ vapor compression systems, Progress in Energy and Combustion Science 30 (2004) 119–174.
[19] O. Fandiño, E.R. López, L. Lugo, J. García, J. Fernández, Solubility of carbon dioxide in pentaerythritol ester oils. New data and modeling using the PC-SAFT model, J. Supercritical Fluids 55 (2010) 62–70.
[20] T. Otsu, H. Tanaka, N. Izumi, J. Sugimura, Effect of surrounding gas on cavitation in EHL, Tribology Online 4 (2009) 50–54.
[21] W.-H. Chen, C.-H. Chen, C.-M.J. Chang, Y.-H. Chiu, D. Hsiang, Supercritical carbon dioxide extraction of triglycerides from *Jatropha curcas* L. seeds, J. Supercritical Fluids 51 (2009) 174–180.
[22] E. Jenab, F. Temelli, Viscosity measurement and modeling of canola oil and its blend with canola stearin in equilibrium with high pressure carbon dioxide, J. Supercritical Fluids 58 (2011) 7–14.
[23] S. Machmudah, M. Kondo, M. Sasaki, M. Goto, J. Munemasa, M. Yamagata, Pressure effect in supercritical $CO_2$ extraction of plant seeds, J. Supercritical Fluids 44 (2008) 301–307.
[24] H. Sovová, M. Zarevúcka, M. Vacek, K. Stránský, Solubility of two vegetable oils in supercritical $CO_2$, J. Supercritical Fluids 20 (2001) 15–28.
[25] T. Klein, S. Schulz, Measurement and model prediction of vapor–liquid equilibria of mixtures of rapeseed oil and supercritical carbon dioxide, Industrial & Engineering Chemistry Research 28 (1989) 1073–1081.
[26] P.M. Ndiaye, E. Franceschi, D. Oliveira, C. Dariva, F.W. Tavares, J.V. Oliveira, Phase behavior of soybean oil, castor oil and their fatty acid ethyl esters in carbon dioxide at high pressures, J. Supercritical Fluids 37 (2006) 29–37.
[27] P.J. Carvalho, J.A.P. Coutinho, On the nonideality of $CO_2$ solutions in ionic liquids and other low volatile solvents, J. Physical Chemistry Letters 1 (2010) 774–780.
[28] L. Zong, S. Ramanathan, C.-C. Chen, Fragment-based approach for estimating thermophysical properties of fats and vegetable oils for modeling biodiesel production processes, Industrial & Engineering Chemistry Research 49 (2010) 876–886.
[29] L. Zong, S. Ramanathan, C.-C. Chen, Fragment-based approach for estimating thermophysical properties of fats and vegetable oils for modeling biodiesel production processes, Industrial & Engineering Chemistry Research 49 (2010) 3022–3023.
[30] F.M. Gaciño, T. Regueira, L. Lugo, M.J.P. Comuñas, J. Fernández, Influence of molecular structure on densities and viscosities of several ionic liquids, J. Chemical & Engineering Data 56 (2011) 4984–4999.
[31] A.M.A. Dias, H. Carrier, J.L. Daridon, J.C. Pàmies, L.F. Vega, J.A.P. Coutinho, I.M. Marrucho, Vapor–liquid equilibrium of carbon dioxide–perfluoroalkane mixtures: experimental data and SAFT modeling, Industrial & Engineering Chemistry Research 45 (2006) 2341–2350.
[32] J. Pauly, J. Coutinho, J.-L. Daridon, High pressure phase equilibria in methane + waxy systems: 1. Methane + heptadecane, Fluid Phase Equilibria 255 (2007) 193–199.
[33] P.J. Carvalho, V.H. Álvarez, J.J.B. Machado, J. Pauly, J.-L. Daridon, I.M. Marrucho, M. Aznar, J.A.P. Coutinho, High pressure phase behavior of carbon dioxide in 1-alkyl-3-methylimidazolium bis(trifluoromethylsulfonyl)imide ionic liquids, J. Supercritical Fluids 48 (2009) 99–107.
[34] G. Soave, Equilibrium constants from a modified Redlich–Kwong equation of state, Chemical Engineering Science 27 (1972) 1197–1203.
[35] T. Sankarappa, M. Prashant Kumar, A. Ahmad, Ultrasound velocity and density studies in some refined and unrefined edible oils, Physics and Chemistry of Liquids 43 (2005) 507–514.

[36] T. Regueira, L. Lugo, O. Fandiño, E.R. López, J. Fernández, Compressibilities and viscosities of reference and vegetable oils for their use as hydraulic fluids and lubricants, Green Chemistry 13 (2011) 1293–1302.
[37] L.A. Quinchia, M.A. Delgado, C. Valencia, J.M. Franco, C. Gallegos, Viscosity modification of high-oleic sunflower oil with polymeric additives for the design of new biolubricant formulations, Environmental Science & Technology 43 (2009) 2060–2065.
[38] B. Esteban, J.-R. Riba, G. Baquero, A. Rius, R. Puig, Temperature dependence of density and viscosity of vegetable oils, Biomass and Bioenergy 42 (2012) 164–171.
[39] B. Guignon, C. Aparicio, P.D. Sanz, Volumetric properties of sunflower and olive oils at temperatures between 15 and 55 °C under pressures up to 350 MPa, High Pressure Research 29 (2009) 38–45.
[40] O. Fandiño, J. García, M.J.P. Comuñas, E.R. López, J. Fernández, PρT measurements and equation of state (EoS) predictions of ester lubricants up to 45 MPa, Industrial & Engineering Chemistry Research 45 (2006) 1172–1182.
[41] M. Wesołowski, J. Erecińska, Thermal analysis in quality assessment of rapeseed oils, Thermochimica Acta 323 (1998) 137–143.
[42] L.A. Quinchia, M.A. Delgado, C. Valencia, J.M. Franco, C. Gallegos, Viscosity modification of different vegetable oils with EVA copolymer for lubricant applications, Industrial Crops and Products 32 (2010) 607–612.
[43] O.O. Fasina, Z. Colley, Viscosity and specific heat of vegetable oils as a function of temperature: 35 °C to 180 °C, International J. Food Properties 11 (2008) 738–746.
[44] J. de Dios Alvarado, Propiedades mecánicas de aceites y grasas vegetales, Grasas y Aceites 46 (1995) 264–269.
[45] M. Kumar, P.N. Shankar, The kinematic viscosities of ethylene-glycol and castor-oil, Current Science 65 (1993) 983–984.
[46] H. Noureddini, B. Teoh, L. Davis Clements, Viscosities of vegetable oils and fatty acids, J. American Oil Chemists' Society 69 (1992) 1189–1191.
[47] M.P. Fernández-Ronco, M. Cismondi, I. Gracia, A. De Lucas, J.F. Rodríguez, High-pressure phase equilibria of binary and ternary mixtures of carbon dioxide, triglycerides and free fatty acids: measurement and modeling with the GC-EOS, Fluid Phase Equilibria 295 (2010) 1–8.
[48] T. Regueira, O. Fandiño, L. Lugo, E.R. López, J. Fernández, Carbon dioxide solubility in reference and vegetable lubricants developed for two stroke engines, J. Supercritical Fluids 68 (2012) 123–130.
[49] M. Maiwald, H. Li, T. Schnabel, K. Braun, H. Hasse, On-line $^{1}$H NMR spectroscopic investigation of hydrogen bonding in supercritical and near critical $CO_2$–methanol up to 35 MPa and 403 K, J. Supercritical Fluids 43 (2007) 267–275.
[50] S. Bai, C.R. Yonker, Pressure and temperature effects on the hydrogen-bond structures of liquid and supercritical fluid methanol, J. Physical Chemistry A 102 (1998) 8641–8647.
[51] D.S. Bulgarevich, T. Sako, T. Sugeta, K. Otake, Y. Takebayashi, C. Kamizawa, Y. Horikawa, M. Kato, The role of general and hydrogen-bonding Interactions in the solvation processes of organic compounds by supercritical $CO_2$/n-alcohol mixtures, Industrial & Engineering Chemistry Research 41 (2002) 2074–2081.
[52] M. Kanakubo, T. Aizawa, T. Kawakami, O. Sato, Y. Ikushima, K. Hatakeda, N. Saito, Studies on solute–solvent interactions in gaseous and supercritical carbon dioxide by high-pressure $^{1}$H NMR spectroscopy, J. Physical Chemistry B 104 (2000) 2749–2758.
[53] J.C. Dobrowolski, M.H. Jamróz, Infrared evidence for $CO_2$ electron donor–acceptor complexes, J. Molecular Structure 275 (1992) 211–219.
[54] O. Pfohl, S. Petkow, G. Brunner, Usage of PE A program to calculate phase equilibria, Herbert Utz Verlag, München, 1998, ISBN 3-89675-410-6.
[55] B.E. Poling, J.M. Prausnitz, J.P. O'Connell, The Properties of Gases and Liquids, 5th ed., McGraw-Hill, New York, 2001.
[56] L. Constantinou, R. Gani, New group contribution method for estimating properties of pure compounds, AIChE Journal 40 (1994) 1697–1710.
[57] S. Glisic, D. Skala, The prediction of critical parameters for triolein, diolein, monoolein and methyl esters, 2009, Arcachon, France, May 18–20.